THE ASTROPHYSICAL JOURNAL, 382:134–142, 1991 November 20

CORE MASSES AND ABUNDANCES OF LOW-EXCITATION PLANETARY NEBULAE IN THE MAGELLANIC CLOUDS

JAMES B. KALER
Department of Astronomy, University of Illinois, 103 Astronomy Building, 1002 West Green Street, Urbana, IL 61801
AND
GEORGE H. JACOBY
Kitt Peak National Observatory, National Optical Astronomy Observatories,[1] P.O. Box 26732, Tucson, AZ 85726
Received 1991 January 28; accepted 1991 May 24

ABSTRACT

We derive core masses and chemical compositions for luminous low-excitation planetary nebulae in the Magellanic Clouds. They are all on horizontal (heating) evolutionary tracks with core masses that concentrate between 0.55 and 0.6 $M_\odot$, and have low He/H and N/O ratios as expected from the relation found by Kaler & Jacoby. The behavior of carbon with core mass is uncertain, but it seems consistent with the behavior of carbon stars. There is also a suggestion that C/O anticorrelates with N/O. Below 0.63 $M_\odot$, O/H correlates positively with core mass.

In combination with Kaler & Jacoby, Dopita & Meatheringham, and Aller et al., we now have accurate core masses for 80 planetaries in the Magellanic Clouds. Of these, 33 are members of a bright sample, defined as the set of 50 that fall in the top 1.5 mag of the [O III] luminosity function. We find excellent agreement between the core mass distribution of this group and the prediction of Jacoby that [O III]–bright planetaries have a very narrow Gaussian high-mass cutoff. The distribution of core masses on the log L–log T plane is qualitatively consistent with theoretical evolutionary rates.

Subject headings: galaxies: Magellanic Clouds — nebulae: abundances — nebulae: planetary

1. INTRODUCTION

In a series of three papers (Kaler & Jacoby 1989; Jacoby & Kaler 1989; Kaler & Jacoby 1990, the last hereafter KJ1) we have (1) demonstrated how it is possible to derive accurate temperatures of the nuclei of high-excitation optically thick planetary nebulae without direct observation of the central star; (2) used this technique to find accurate core masses for planetaries with known distances, namely those in the Magellanic Clouds; and (3) determined the relationship that exists between the chemical compositions—and chemical enrichments—of the nebulae and the stellar core masses. In KJ1 we find that as core mass (M_c, always in solar units) increases, the N/O remains at a low level until about 0.65 $M_\odot$, whereupon it suddenly rises to high values, consistent with hot-bottom burning in the envelope. The He/H increases continuously, and above 0.64 $M_\odot$, the C/O appears to be decreasing. However, above about 0.8–1 $M_\odot$ the N/O and He/H do not attain such high levels. A correlation between N/O and core mass is also seen for the Galaxy (Kaler, Shaw, & Kwitter 1990; Stasinska & Tylenda 1990), although it is weaker because of uncertain distances.

KJ1 determined the temperatures of these Magellanic Cloud nebulae from the "crossover method," which uses the He II λ4686/Hβ flux ratio, where nebulae of high optical depth are preselected by strong [O II] λ3727. All of the stars are hot, over 90,000 K, ranging up to over 200,000 K, and all are on, or are at least close to, descending (cooling) evolutionary tracks. As a result (a matter to which we will return below), the core masses range to rather high values, enough so as to allow us to see a number of highly enriched nebulae. As always, however, the data are in limited supply. So in this paper we extend the study to low-excitation planetaries, those in which the He II λ4686 line is either absent or very weak, whose core masses can also be derived without direct observations of the nuclei. For these objects, in which the nuclear temperatures are generally less than 60,000 K, the strength of the [O III] λ5007 line [more specifically the λ5007 intensity, 100[$F(\lambda5007)/F(\mathrm{H}\beta)$] is very responsive to temperature. Kaler & Jacoby (1991, hereafter KJ2), improving on Kaler (1978a), correlated $I(\lambda5007)$ with Kaler's (1976) Stoy (energy balance) temperatures and showed that they are the best to use, probably superior to the Zanstra temperatures, which are subject to problems involving optical depth and possible ultraviolet excesses. We now proceed to apply this correlation to the nebulae of the Magellanic Clouds, which allows us again to derive accurate temperatures, luminosities, and core masses.

2. NEBULAR AND STELLAR PARAMETERS

The relation that KJ2 derived for the Galaxy is not directly applicable to the Clouds because of their generally lower O/H ratios. The λ5007 line (along with its companion λ4959) is usually the greatest nebular coolant because of the high abundance of oxygen and the efficiency of the atomic transition causing it. A reduction in O/H would by itself produce a decrease in the λ5007 strength. The reduction in the cooling rate, however, causes an increase in the electron temperature, which in compensation raises the λ5007 intensity. To a coarse degree, then, the strength of this line is independent of O/H. However, the compensation cannot be complete, and we in fact witness a small weakening of λ5007 as O/H goes down. Consequently, before we can apply the KJ2 relation to the Cloud objects, we must first find the mean electron temperatures and

[1] The National Optical Astronomy Observatories are operated by the Association of Universities for Research in Astronomy, Inc., under cooperative agreement with the National Science Foundation.

chemical compositions of our sets of nebulae so that we may correct it.

2.1. *Chemical Compositions*

We make use of three data sets, two large ones from Monk, Barlow, & Clegg (1988, hereafter MBC) and Meatheringham & Dopita (1991, hereafter MD), and a small one from Aller et al. (1981). In addition, we include one observation from Aller (1983a). We selected only the objects for which the mean He II λ4686 intensity is less than 10 (for all but one nebula it is effectively zero). They are listed in Table 1; just over half were observed at least twice by either the same or by different

TABLE 1

CHEMICAL COMPOSITIONS OF MAGELLANIC CLOUD PLANETARY NEBULAE

Nebula (1)	T_e[O III][a] (2)	T_e[N II][a] (3)	$10^3 N_e$ (4)	10^4 O/H (5)	He/H (6)	N/O (7)	C/O (8)	References (9)
Large Magellanic Cloud								
SMP 1	11250	13170*	3.6	2.15	0.086	0.22	...	1
	11180	13180*		1.88	0.133	0.38	0.59	2
SMP 3	15670	11110*	39.4	>0.45	0.074	...	...	1
SMP 5	13160*	10320*	2.0	1.17	0.087	0.05	...	1
	13160	10300*		1.26	0.064	0.02	...	2
SMP 8	10800*	11990*	4.8	1.72	0.119	0.28	...	1
	10800	11990*		1.66	0.140	0.83	...	2
SMP 23	12580	13100*	4.3	1.57	0.075	...	...	1
	11230	13130*		2.14	0.082	0.10	...	2
	11703	11300*		1.88	0.101	0.08	...	3
SMP 31	12410*	19160*	11.2	0.19	0.029	0.44	...	1
	12410*	19060*		0.22	0.063	0.83	...	2
SMP 48	11170	12650*	9.4	1.98	0.086	0.22	...	1
SMP 55	12640*	10000	27.2	1.44	0.059	0.15	...	1
	12640	11610		1.22	0.070	0.12	...	2
SMP 56	12980	10250*	5.0	1.16	0.082	0.03	...	2
SMP 58	12480	12730*	66	1.59	0.074	0.11	...	1
	11540	11300*		2.08	0.090	0.08	11.7	2
SMP 61	10250	10520*	35	4.18	0.096	0.04	...	1
	11030	10520*		3.43	0.114	0.07	2.4	2
SMP 63	11480	13850*	8.8	2.51	0.085	0.34	...	1
	11510	13820*		2.50	0.101	0.22	...	2
SMP 65	10590	12880*	5.0	2.38	0.110	...	...	2
SMP 67	12290	10730	3.7	1.06	0.112	0.68	...	2
SMP 76	10920	12470*	16.7	1.89	0.084	...	...	1
	11210	12130*		1.71	0.096	0.12	3.0	2
SMP 77	11310	10580*	4.3	1.26	0.117	0.11	...	2
SMP 84	13860	13030*	5.0	1.24	0.101	0.08	...	1
SMP 85	11090	12180	10	1.14	0.091	0.32	4.7	2
Small Magellanic Cloud								
SMP 1	10660	10720*	9.7	0.86	0.086	0.12	...	1
	10660	10640*		0.82	0.066	0.13	...	1
	10660	11190*		0.96	0.067	0.17	...	2
SMP 6	14250	18740*	26.7	1.13	0.096	0.70	...	1
	15270	18740		1.01	0.084	0.59	...	1
SMP 7	17800	14950*	2.0	0.91	0.083	0.20	...	2
SMP 8	12990	13520*	5.0	1.13	0.089	...	...	1
SMP 10	10680	14210*	2.2	2.38	0.073	...	...	1
SMP 11	12360*	11530*	2.8	1.23	0.065	...	...	1
SMP 13	12980	14490*	4.5	1.53	0.075	...	...	1
	13510	14510*		1.36	0.099	0.13	1.0	2
SMP 15	12490	12350*	37	1.37	0.081	...	2.9[b]	1
	11410	12350*		1.66	0.095	0.14	1.5	2
SMP 16	11590*	10400*	10.2	1.43	0.064	0.03	...	1
	11580	10470*		1.12	0.057	0.03	...	2
SMP 17	12470	14730	4.9	1.78	0.082	...	7.9[b]	1
SMP 18	10240	11410*	22	1.89	0.079	0.03	...	1
SMP 20	11680	12040*	10.5	0.92	0.130	...	4.9[b]	1
	13250	12170*		0.72	0.083	0.14	...	4
SMP 24	12240	14500*	8.4	1.04	0.069	0.20	...	1
	10920	12220*		1.45	0.091	0.10	...	4
SMP 27	13010	13440*	5.9	1.11	0.094	0.11	...	1
	12210	13100*		1.21	0.086	0.12	...	4

[a] Estimated values are indicated by an asterisk.

[b] *IUE* results from Aller et al. 1987.

REFERENCES.—(1) Monk, Barlow, & Clegg 1988; (2) Meatheringham & Dopita 1990; (3) Aller 1983a; (4) Aller et al. 1981.

authors. The analysis was carried out according to the procedure and code (ABUNDR) described by Kaler (1985) and KJ1. Except for the four nebulae observed by Aller et al. (1981) and Aller (1983a), all the data are presented by the authors as corrected for interstellar extinction; the extinctions for the errant four (with corrections applied according to the reddening function of Whitford 1958) are presented in Table 2 below.

T_e[O III] (col. [2] of Table 1) can be calculated for all the nebulae from one data set or another except for SMC/SMP 11, for which 12360 K was adopted (scaled upward from Kaler 1986 to account for lowered mean O/H). If this temperature cannot be calculated for a nebula from one data source (usually MBC) it was adopted from the other and noted by an asterisk. Conversely, only seven nebulae have T_e[N II] (col. [3]). For these we had to adopt values appropriate to a preliminary value of central star temperature from Kaler's (1978a) relation between T_* and $I(\lambda 5007)$ scaled upward by 10% and 20% respectively for the LMC and SMC (see KJ1). These are again indicated by asterisks. Also needed for the analysis are the electron densities. These are all from [O II], are taken from MBC and MD, and are given in column (4).

The resulting O/H, He/H (with the exception of LMC/SMP 58 equal to He^+/H^+), and N/O (set as usual equal to N^+/O^+) are given in the next three columns. The following column gives C/O, calculated either from C II λ4267 and Kaler's (1983a) algorithm or taken from Aller et al.'s (1987) *IUE* study. Finally, the source of the data is indicated in the last column.

2.2. *Core Masses*

In order to derive the core masses of the planetaries we need temperatures (T_*), luminosities (L_*), and a set of evolutionary tracks on the log L–log T plane for stars of different masses. We assume for the sake of calculation that all the nebulae are optically thick, that is, that all the ionizing ultraviolet radiation is absorbed, and return to the problem in the discussion in § 3.1. The stellar temperatures are derived from the strength of λ5007 as described below, and the luminosities from temperatures, the Hβ fluxes, and the distances. In addition, both T_* and L_* depend on the determination of the amount of interstellar extinction along the line of sight.

All the necessary parameters are presented in Table 2, where columns (2), (3), and (4) give, respectively, the extinction constant (c, the logarithmic extinction at Hβ), the logarithm of the Hβ flux, $-\log F(\mathrm{H}\beta)$, and the intensity of [O III] λ5007. The extinctions (calculated from Balmer decrements) are all from MD except for SMC/SMP 20, 24, and 27, which are calculated from Aller et al. (1981). Those for which only Hβ, Hγ, and Hδ were available for use are indicated by footnote c. MBC does not provide extinctions, as the reddening corrections are intrinsic to their reduction procedure. If the extinction was not measured for an object (and the entry is blank in col. [2]) we use means of 0.21 for the LMC and 0.14 for the SMC in accord with KJ1 supplemented by the measured extinctions in Table 1 (excluding a pair of anomalously high values). The Hβ fluxes are taken from Webster (1969, 1983), Wood et al. (1987), and Meatheringham, Dopita, & Morgan (1988), to which we add -0.02 in the log to place them on the modern photometric system (see KJ2), and which we correct for interstellar extinction. LMC/SMP 3 and 8 were corrected for typographical errors found in Meatheringham, Dopita, & Morgan (1988) as reported by Jacoby, Walker, & Ciardullo (1990). The λ5007 intensities are also taken from MBC, MD, and Aller et al. (1981), and Aller (1983a), and are also corrected for interstellar extinction.

TABLE 2

CENTRAL STAR PARAMETERS OF MAGELLANIC CLOUD PLANETARY NEBULAE

Nebula (1)	c (2)	$-\log F(\mathrm{H}\beta)$[a] (3)	$I(\lambda 5007)$[a] (4)	T_* (5)	$L_*/L_\odot$ (6)	M_c (7)
Large Magellanic Cloud						
SMP 1	0.17	12.32	801	64000	3970	0.59
SMP 3	...	12.29[b]	398	44000	5360	0.60
SMP 5	0.83[c]	12.04	272	37000	12100	0.70
SMP 8	0.23	12.53[b]	551	53000	2650	0.57
SMP 23	0.06	12.64	786	64000	1900	0.56
SMP 31	...	12.72	66	28000	4890	0.59
SMP 48	...	12.27	685	60000	4550	0.59
SMP 55	0.26	12.42	148	31000	7210	0.63
SMP 56	0.11[c]	13.04	263	37000	1230	0.55
SMP 58	0.29[c]	12.21	702	60000	5200	0.60
SMP 61	0.19	12.28	720	61000	4410	0.59
SMP 63	0.23	12.26	976	69000	4510	0.59
SMP 65	0.08	13.25	734	62000	470	0.53
SMP 67	0.15	12.68	269	37000	2780	0.57
SMP 76	0.35	12.21	614	56000	5360	0.60
SMP 77	0.26	12.54	313	40000	3480	0.58
SMP 84	...	12.44	768	63000	3020	0.57
SMP 85	0.26	12.18	338	41000	7610	0.64
Small Magellanic Cloud						
SMP 1	0.24[c]	12.54	218	35000	5780	0.61
SMP 6	...	12.68	782	64000	2290	0.57
SMP 7	0.07	12.63	934	68000	2540	0.57
SMP 8	...	12.62	630	57000	2730	0.57
SMP 10	...	12.81	767	63000	1700	0.56
SMP 11	...	12.81	311	40000	2480	0.57
SMP 13	0.43[c]	12.37	829	65000	8070	0.65
SMP 15	0.17	12.28	597	55000	6060	0.61
SMP 16	0.72[c]	12.03	163	32000	22100	0.86
SMP 17	...	12.39	881	67000	4420	0.59
SMP 18	...	12.53	294	39000	4890	0.60
SMP 20	0.03	12.43	397	44000	3890	0.59
SMP 24	0.00	12.72	435	46000	2500	0.57
SMP 27	0.03	12.45	587	55000	4120	0.59

[a] Corrected for interstellar extinction.

[b] Published Hβ flux increased by a factor of 10 (Jacoby, Walker, & Ciardullo 1990).

[c] Hα saturated.

To derive the masses of the planetary nuclei we start with the relation between $I(\lambda 5007)$ and the Stoy temperature defined by KJ2, viz.

$$T_S = 25840 + 19.30I + 0.028229I^2 - 1.46115 \times 10^{-5} I^3 . \quad (1)$$

This equation was derived for the Galaxy and is clearly sensitive to the O/H ratio and must be corrected for the different abundances in the Clouds. For any given stellar temperature, a lower O/H results in a reduced λ5007 intensity. But lower O/H increases the electron temperature, which will raise the λ5007 intensity. The intercept of 25,840 K is the central star temperature for which the λ5007 line will disappear and is independent of O/H, that is, O^{2+} should go to zero at that point no matter what the total oxygen abundance; the result is that only the coefficients would be affected by a change in O/H. The factor by which the coefficients of equation (1) should be multiplied is equal to the factor by which O/H is depressed multipled by the factor by which λ5007 is increased as a consequence of the observed increase in T_e[O III].

The O/H derived from planetaries in the Clouds is different from that found for H II regions and can differ from one set of planetaries to another (see, for example, KJ1 and references therein), so that we must correct the calibration for this particular set of objects. Lower excitation Galactic planetaries have a strong admixture of Population II and an O/H ratio that is lower than solar or that found in the Galactic disk. About half of the KJ2 sample, from which equation (1) was constructed, has O/H available from Kaler (1981), from which we find a mean value of 3.44×10^{-4}. From Kaler (1986) we also find a mean T_e[O III] for the same objects of 10,500 K. The mean O/H ratios for the LMC and the SMC from Table 1 are 1.68×10^{-4} and 1.34×10^{-4}, respectively, and the mean electron temperatures are 12,000 and 12,500 K. The differences between low-excitation planetaries in the two Clouds are so small that we combine them, with O/H reduced by a factor of 2.28 and the electron temperature raised from 10,500 to 12,250 K; the latter corresponds to an increase in $I(\lambda 5007)$ of a factor of 1.55. The result is that the coefficients of the intensities in equation (1) must be increased by a factor of 1.5^n, where n is the power to which I is raised, which is in excellent agreement with the factor of 1.51 found by adopting Jacoby's (1989) recommendation that $I(\lambda 5007)$ scales as $(O/H)^{1/2}$, found by using the nebular models of Aller & Keyes (1987). The result for the Magellanic Clouds is then

$$T_* = 25840 + 28.95I + 0.0635I^2 - 4.931 \times 10^{-5} I^3 . \quad (2)$$

The resulting values of T_* are placed in column (5) of Table 2. The stellar luminosities, given in column (6), follow immediately from the temperatures and the Hβ fluxes, where we adopt distances of 50.1 and 57.5 kpc for the LMC and SMC as in KJ1. In practice we simply substitute the temperatures into the Zanstra code described by Kaler (1983b). In Figure 1 we then place all the stars on the same log L–log T plane used by KJ1 (which uses evolutionary tracks from Wood & Faulkner 1986; Paczyński 1971; and Schönberner & Weidemann 1981), which allows us to determine the core masses (col. [7]).

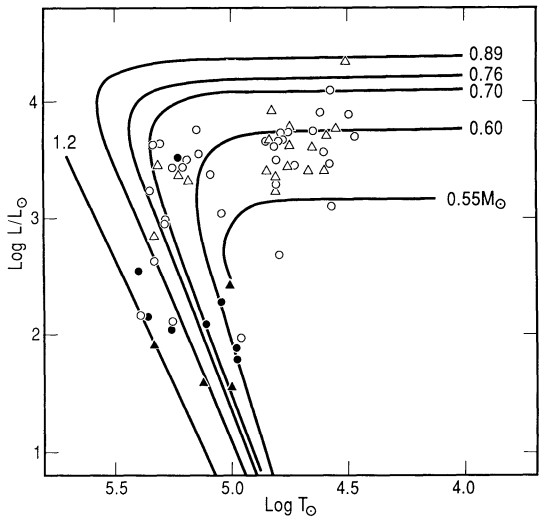

FIG. 1.—Magellanic Cloud planetary nuclei on the log L–log T plane. The new data are superposed on the original figure by KJ1 and are all clustered below log $T = 4.9$. The stars from the LMC and SMC are shown respectively as circles and triangles. The filled points are placed with absolute fluxes from Boroson & Liebert (1989).

Equation (2) is not the same as used for the estimation of [N II] electron temperature in the abundance code (see § 2.1). Those were recalibrated in a different way by KJ1, and it is best if we use the same procedure here so that our new results can consistently be compared with theirs. Given the possible errors in the estimation of T_e[N II], the difference is of little consequence.

3. RESULTS

3.1. *Temperatures and Optical Depth*

Dopita & Meatheringham (1991, hereafter DM) have calculated the effective temperatures of several of the stars considered here by means of a detailed photoionization model. We plot our temperatures from Table 2 against theirs (T_{DM}) in Figure 2 where we see that the two are very nicely correlated with one another but with an offset from the 45° line. We can divide the figure into three distinct temperature regions: $T_{DM} < 50{,}000$ K, $50{,}000 < T_{DM} < 70{,}000$ K, and $T_{DM} > 70{,}000$ K. In the lowest temperature range, ours is an average of 17% or 6000 K less than theirs. In the middle range the fit is excellent, ours being only 1% higher. Then in the upper range ours are again depressed, now by 28% or 21,000 K. One possible explanation for the difference is low optical depth in the nebulae. The photoionization technique should be independent of optical depth, whereas the Stoy method (on which the T_*-$\lambda 5007$ relation is based) will yield lower (but close) limits if the nebulae leak radiation. KJ2 showed that as T_* increases from the minimum, the Galactic planetaries begin as optically thick and then tend to become, or are allowed to become, optically thin somewhere in the 40,000–50,000 K range. Note, however, that the T_* depression relative to T_{DM} is worse in the lower temperature range and that the two tend toward agreement in the 50,000–60,000 K range, opposite to the expected behavior. We therefore conclude that below 70,000 K, optical depth is of little consequence in terms of our results. The offset in Figure 2 could be due to systematic errors in the original Stoy temperatures (see KJ2), in the correction of the KJ2 calibration to the Clouds, or even in the technique used to calculate the photoionization temperatures, T_{DM}. It seems quite

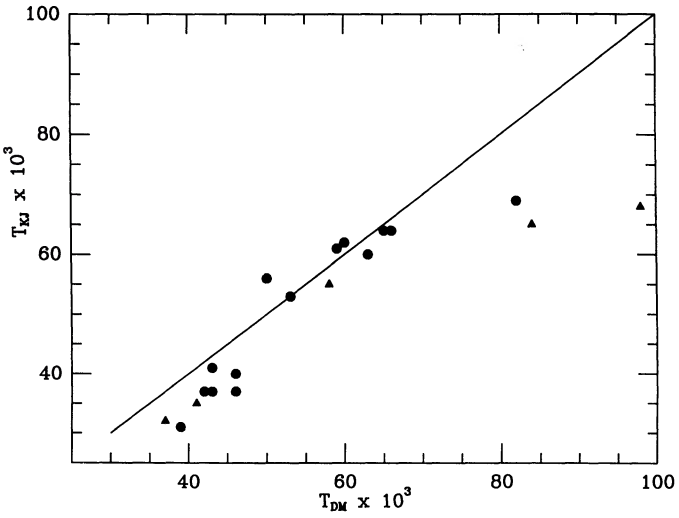

FIG. 2.—Our temperatures, T_*, from Table 2 plotted against those from Dopita & Meatheringham (1991), T_{DM}. LMC and SMC stars are plotted as circles and triangles, respectively. The 1:1 line is included for reference.

possible that the three hot objects, those with $T_{DM} > 70{,}000$ K (LMC/SMP 63, SMC/SMP 7 and 13), are optically thin, although the lack of nebular He II λ4686 for LMC/SMP 63 and SMC/SMP 13 (see MD) is inconsistent with the high T_{DM}. In general, the comparison supports our method.

3.2. *Distribution on the log L–log T plane*

Note in Figure 1 the very different distributions of stars between that found in KJ1 and that found from the present data set. The bright stars of the low-excitation nebulae—those on the horizontal or heating tracks—have low masses that concentrate between 0.55 and 0.6 $M_\odot$, whereas those hot stars on the descending or cooling tracks have masses that range upward from 0.6 $M_\odot$ to quite high values. The overall distribution, which shows the points skewed across the log L–log T plane toward higher masses at greater ages and lower luminosities, is quite in accord with what is expected from theoretical evolutionary ages; see, for example, Wood & Faulkner (1986). The distribution looks qualitatively very much like that calculated with theoretical ages by Shaw (1989). Higher mass cores evolve very quickly along the heating tracks across the top of the diagram so that we selectively see only those of lower mass that are evolving much more slowly. The higher mass cores then greatly slow their evolutionary rates as they cool, and we selectively find them when they are faint and their nebulae have grown large.

This difference is the reason for some of the controversy concerning the general distribution of central star masses, and is why those authors who select the common bright nebulae in the Galaxy find narrow core mass distributions (e.g., Schönberner 1981) and those that look at large objects find a broader range (e.g., Kaler 1983). There is little point in making any further or quantitative comparisons between theory and observation since we do not have a complete sample of nebulae in Figure 1, nor are the calculated evolutionary rates correct in detail (see Kaler et al. 1990).

Nevertheless, it is possible to make one comparison by choosing a magnitude-limited subset of the objects in accord with the selection criteria used for extragalactic distance scale studies. In Figure 3, we have plotted the core mass distribution based on the 32 objects in this study, the 32 objects from KJ1, and 16 additional objects from DM and Aller et al. (1987). Also in Figure 3, we show the distribution of 33 objects that remain after rejecting all of those having [O III] λ5007 luminosities more than 1.5 mag fainter than the upper luminosity limit defined by Ciardullo et al. (1989). There are a total of 50 planetaries in the Clouds that satisfy this constraint (Jacoby et al. 1990), and so we have masses for over half the sample. Fainter objects have little weight in the modeling procedure used by Jacoby (1989), and so should not be considered in the comparison.

Note that all the high-mass objects in the upper panel of Figure 3 have been removed from the sample in the lower panel, in good agreement with the prediction of Jacoby (1989) that a cutoff in core mass exists for [O III]–bright nebulae. The distribution is similar to that found for the Galaxy by Tylenda et al. (1991). We can derive the cutoff rate directly from the observations. In Figure 4, we plot mass cutoffs assuming the Gaussian parameter, sigma, to be 0.02, 0.04, and 0.06 $M_\odot$. Although the small number of objects limits the accuracy of comparison, we tentatively adopt the middle case as the best.

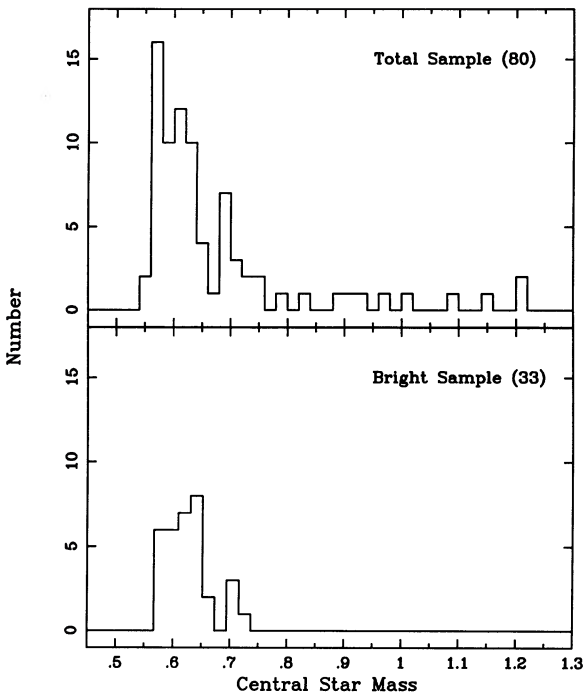

FIG. 3.—The number distribution of core masses placed in 0.02 $M_\odot$ bins for the 80 MC PN from KJ1, this paper, DM, and Aller et al. (1987). Average masses are used when overlap exists. The upper panel shows all available data. The lower panel shows the subset in which all [O III]–faint planetary nebulae have been excluded.

It would seem that a sigma of 0.04 $M_\odot$ is large compared to Jacoby's (1989) prediction of 0.02 $M_\odot$, but it is evident that both values are small in an absolute sense. Furthermore, observational uncertainty (estimated to be 0.03 $M_\odot$ by KJ1) must be deconvolved from the value of 0.04. Subtracting in quadrature, we find that the intrinsic cutoff in Figure 4 can be approximated by a Gaussian with sigma $\approx$ 0.03 $M_\odot$.

Thus, the core masses derived for planetary nebulae in the Magellanic Clouds support the claims for using the nebulae as

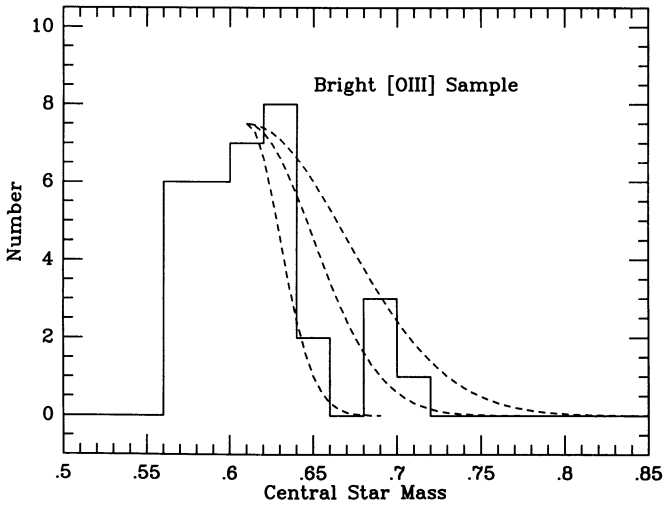

FIG. 4.—The same as the lower panel of Fig. 3, but we have overplotted dotted lines representing Gaussian cutoffs centered at 0.61 $M_\odot$ and having σ = 0.02, 0.04, and 0.06 $M_\odot$.

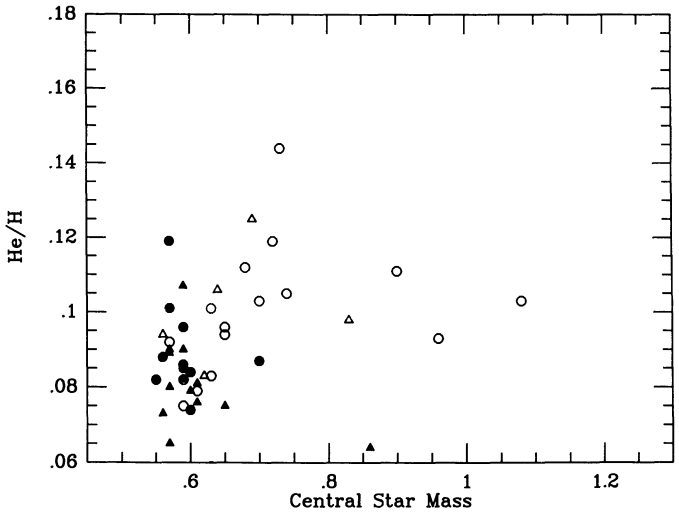

FIG. 5.—He/H plotted against core mass, M_c, which is in solar units. The KJ1 results are plotted as open symbols, with LMC and SMC objects represented by circles and triangles, respectively. The He/H ratios from the MBC and Aller et al. (1981) data sets are similarly plotted as filled symbols.

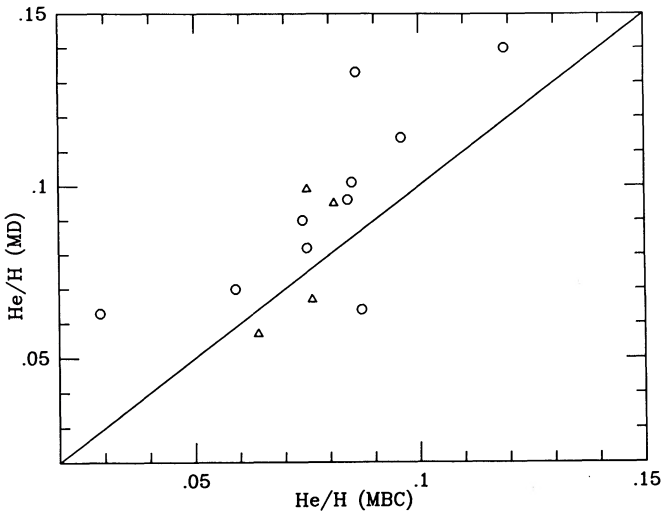

FIG. 6.—He/H from the MD data set plotted against that from the MBC set. LMC and SMC objects are plotted as circles and triangles, respectively.

standard candles in deriving extragalactic distances. It remains something of an open issue as to why planetaries having high core mass are not seen as bright objects in [O III], although Jacoby (1989) discusses some possible causes (e.g., evolutionary rates of the horizontal tracks than are more rapid than models predict).

3.3. *Helium*

KJ1 showed that for central stars with core masses below 0.8 $M_\odot$, He/H ratios climb continuously with increasing core mass, from a low of about 0.08 to about 0.11. Their results are replotted in Figure 5 as open symbols. We have a special problem with these low-excitation objects because the lower star temperatures can lead to significant amounts of neutral helium, giving the impression of He/H ratios that are too low. Kaler (1978b) showed that for Galactic nebulae, neutral helium is not important for $T_* > 45{,}000$ K, which appears to be consistent with the He/H ratios in Table 1. We consequently reject those values for which T_* is less than 45,000 K (unless they are unusually high).

The change in He/H with M_c is small, and it is necessary to have rather accurate line intensities to see it. If we plot the mean He/H ratios against core mass, the correlation becomes badly smeared, that is, there are a number of low-mass stars with rather high average He/H ratios. Figure 6, however, shows that there is an obvious difference between the He/H found from the MBC and MD data (where here we include all the objects regardless of T_*), with the latter systematically high by an average of 20%. The problem obviously must lie in systematic differences in the He I line intensities, which are plotted (I_{MD} against I_{MBC} for He I λ4471, λ6678, λ5876) in Figure 7, where the differences, especially in the λ5876 line, are readily apparent. Are the MD intensities overestimated or are the MBC intensities underestimated? We compare the MBC He/H ratios with those of Aller (1983a) for LMC/SMP 23 and Aller et al. (1981) for SMC/SMP 20, 24, and 27, which we supplement with four nebulae (LMC/SMP 21, 78, 83, and SMC/SMP 5) that were studied by KJ1 and observed by both MBC and others, and find that on average, the combined Aller data give values that are only 6% high relative to those from MBC, suggesting that the MD intensities may be too strong. However, the number of data points is small, and the systematic effect between MD and MBC rests mainly on only a few objects for which the differences are large, so that any judgments are compromised.

In any case, because we used the MBC data in the original correlation in KJ1, consistency demands that we continue to use them here. We therefore exclude the MD helium data, but add the data from Aller (1983a) and Aller et al. (1981), since they seem to agree reasonably well with MBC. We plot the He/H from these sources only (the means where appropriate) in Figure 5 as closed circles and triangles for the LMC and SMC, respectively, where we see that on the whole they are consistent with KJ1's conclusions.

There are a few renegades in Figure 5, however: the He/H ratios for LMC/SMP 5 and SMC/SMP 13, at 0.70 and 0.65 $M_\odot$, are too low, and those for SMC/SMP 20 (0.59 $M_\odot$), and

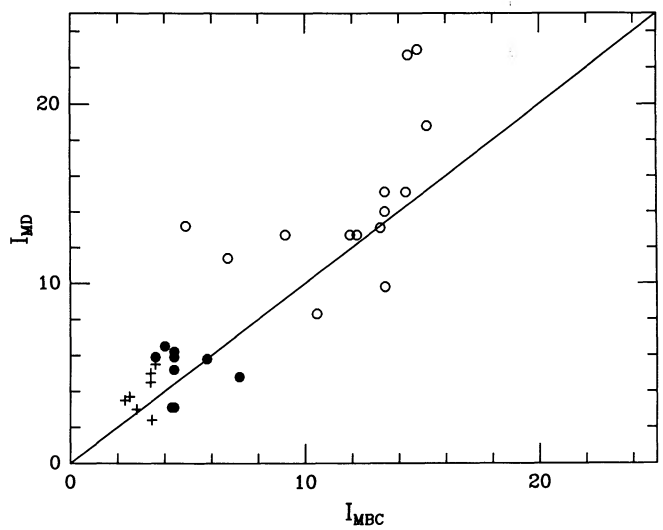

FIG. 7.—He I line intensities from MD plotted against those from MBC. *Open circles:* λ5876; *crosses:* λ6678; *closed circles:* λ4471.

LMC/SMP 8 and possibly 84 (both 0.57 $M_\odot$) are too high. We may be able to discount four of the five. Hα was saturated in the spectra acquired for LMC/SMP 5 and SMC/SMP 13, and the extinctions were derived from Hβ, γ, and δ. Because of the short wavelength base, they are subject to higher error. Note in Table 2 that of those marked with footnote c, two extinctions are anomalously high. In fact in MD's whole data set, of those with good Hα only 2 of 30 nebulae have $c > 0.50$, whereas with those with saturated Hα, four of 10 fall into that category. However, note also that this relation may be due to a selection effect. If an observer exposes long enough to reach the blue lines of a heavily reddened nebula, the red lines will appear very strong and may thus become saturated. Even so, if Hα is not available, the extinctions are subject to higher error. Perhaps, then, the extinction for LMC/SMP 5 and SMC/SMP 13 are too high, leading to erroneously high core masses. If we reduce c to 0.19, they drop to 0.57 and 0.60, respectively, which would make them fit. In addition, there is no measured extinction for LMC/SMP 84. If it is higher than average, the mass would be higher, and the point could fit. Finally, SMC/SMP 20 has two very different values of measured He/H and a very high associated error. If we use only the Aller et al. (1981) data, He/H drops to 0.083, in good accord with the correlation. That leaves LMC/SMP 8, which is a clear anomaly. All these objects need further study.

3.4. *Nitrogen*

The N/O ratios show no significant systematic differences among authors. Here, however, we run into a different problem in that the [N II] electron temperatures that are critical for accurate assessments of the nitrogen abundances are known only for five of the 32 nebulae considered: all the rest are estimates and could be wrong by a large amount. Moreover, young objects tend to be quite dense, with several above 10^4 cm^{-3}, in the density region where the [O II] lines do not produce accurate values. In Figure 8 we replot N/O against M_c from KJ1 as open circles and triangles (for the LMC and SMC, respectively) and add the mean N/O ratios from this paper as closed symbols, where we reject all the nebulae with $N_e > 10^4$ cm^{-3}.

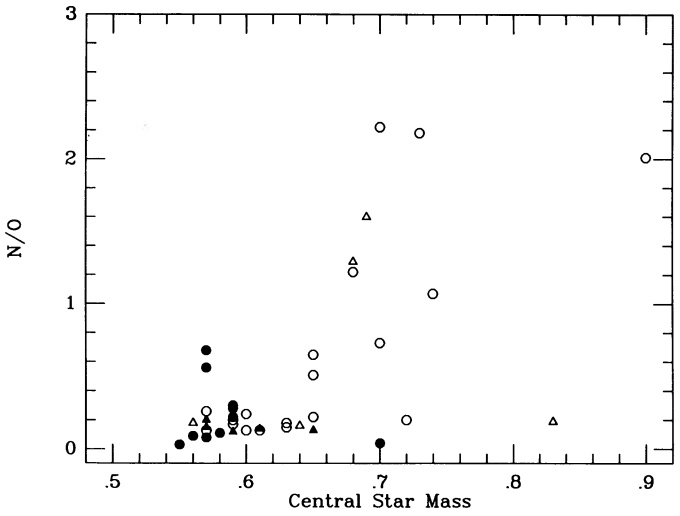

FIG. 8.—N/O ratios plotted against core mass, M_c, where circles and triangles respectively represent the LMC and SMC. The open and closed symbols are taken from KJ1 and this paper, respectively.

We see that with the exception of LMC/SMP 67 and *again* LMC/SMP 8, the new low-mass cores have nebulae with low N/O. The two available N/O measurements for SMP 8 are quite different, and we can alleviate the discrepancy by choosing that calculated from MBC's data. It could be lowered further by reducing the uncertain electron temperature. SMP 67 is the outstanding anomaly here, as it has a low and reliable density and is one of the few with measured T_e[N II]. (Note also that if we had used MD's data in the He/H correlation that SMP 67 would be anomalous there as well.) Another possible exception to the correlation is LMC/SMP 5, which has a low N/O for its mass of 0.70 $M_\odot$ (although KJ1 do show a few others in this region of the diagram). However, this nebula has a very high extinction and Hα was again saturated, suggesting that the core mass may be overestimated. Although the point is not plotted because the electron density is too high, the same may be said of SMC/SMP 16. It has the distinction of having the highest measured core mass and lowest N/O (see the Tables). Even if we were to lower N_e by an order of magnitude and increase T_e to 15,000 K we could raise N/O only to 0.09. This nebula is again one of those with saturated Hα and a very high extinction; M_c could be markedly lowered by decreasing c. Low optical depth may exacerbate the problem (see § 3.2); if we use Dopita & Meatheringham's (1991) temperature, the core mass falls to 0.75 $M_\odot$.

We conclude that the new results are consistent with the relation found by KJ1 and confirm the prediction originally made by Renzini (1979) that high N/O objects should selectively be found among the nebulae with the fainter stars that are on descending, or cooling, evolutionary tracks. However, again note the exceptions: LMC/SMP 8 and 67 bear close scrutiny. High helium and nitrogen abundances are known among Galactic Population II planetaries, which are presumably also of lower mass (see Kaler 1978b: Me 2-2 is a case in point); perhaps there is a relation.

3.5. *Carbon*

KJ1 suggested—from a sparse four planetaries—that above 0.63 $M_\odot$, C/O anticorrelates with core mass and declines as N/O increases. We can add here to the number of points and include several of lower mass to see—possibly—where C/O begins to increase and where it reaches a maximum. The C/O ratios from Table 2 are plotted against core mass in Figure 9, where the Large and Small Clouds are again discriminated by circles and triangles; the C/O derived from ultraviolet (*IUE*) data are indicated by filling the symbols. Above 0.63 $M_\odot$ we add two new points (given the error inherent in M_c) are consistent with the decline as M_c increases. The others tend to scatter, and no clear trend is readily obvious from the figure alone. However, on the basis of the observations of carbon stars, particularly those in the Clouds (see, e.g., Iben 1988), we would expect a rise with M_c as the carbon dredge-up phenomenon begins followed by a fall as the initial mass (and the core mass) increases beyond a critical limit. The distribution in Figure 7 is at least consistent with this picture, with C/O beginning to increase around 0.60 $M_\odot$ or below. The maximum appears to be somewhere in the 0.60–0.63 $M_\odot$ range.

A plot of C/O versus N/O (Fig. 10) shows perhaps a better relation. Here we plot all the data regardless of electron density and indicate those with $N_e > 10^4$ cm^{-3} by a slash. There appears to be an anticorrelation, with C/O low for any objects in which N/O is significantly high, and N/O low when C/O is high. It is best seen if only the more reliable results from *IUE*

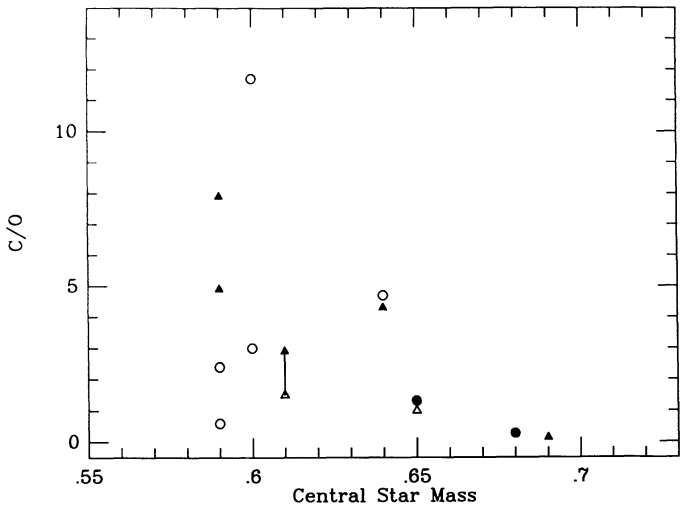

FIG. 9.—C/O ratios plotted against core mass, M_c. Circles and triangles represent LMC and SMC objects as before. Ratios determined from *IUE* data are filled. The optical and ultraviolet results for SMC/SMP 15 are connected by a vertical bar.

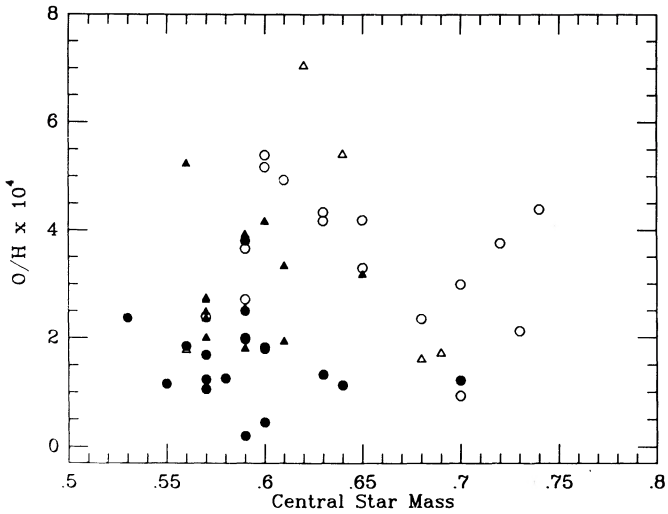

FIG. 11.—O/H plotted against core mass. The open circles and triangles are from KJ1, and the filled circles are from this paper. O/H for SMC objects are multiplied by a factor of 2.2 to remove the effect of gross metallicity differences between the two clouds.

are considered. Unfortunately, the number of nebulae available is quite low. Clearly, a proper study of C/O ratios will take much more observations.

3.6. *Oxygen*

It has become clear over the years that oxygen abundances are somehow linked to the dredge-up phenomena that affect nitrogen, helium, and carbon, as O/H is anticorrelated with N/O (Aller 1983b; Torres-Peimbert 1983; Henry, Liebert, & Boroson 1989; Kaler et al. 1990; KJ1). In Figure 11 we combine the O/H from this paper with the values from KJ1 and plot them against core mass, where we reveal another possible, potentially important, aspect of the subject. In order to reduce confusion, and to improve the prospects for seeing a correlation, we scale the individual SMC oxygen abundances to those of the LMC by multiplying all the former by 2.2, the ratio of mean oxygen abundances found in KJ1. As M_c increases from $\approx 0.55\ M_\odot$ to $\approx 0.63\ M_\odot$, O/H correlates positively at the 98% confidence level. We note that statistical confidence level tests are useful only to reject a correlation. Thus, we conclude that there is no correlation between M_c and O/H above about $0.63\ M_\odot$. However, below that mass, we cannot reject the possibility that abundance enhancements correlate with core mass. The correlation results from the low incidence of high O/H for stars having core masses less than $0.59\ M_\odot$ relative to those with core masses greater than that value. A truly random distribution does not have a void. We also note that a similar correlation is found for the Galaxy by Stasinska & Tylenda (1991).

Clearly this possible correlation needs to be examined further in order to test its reality, since if it is real, it bears powerfully on the matter of internal processes in giant stars.

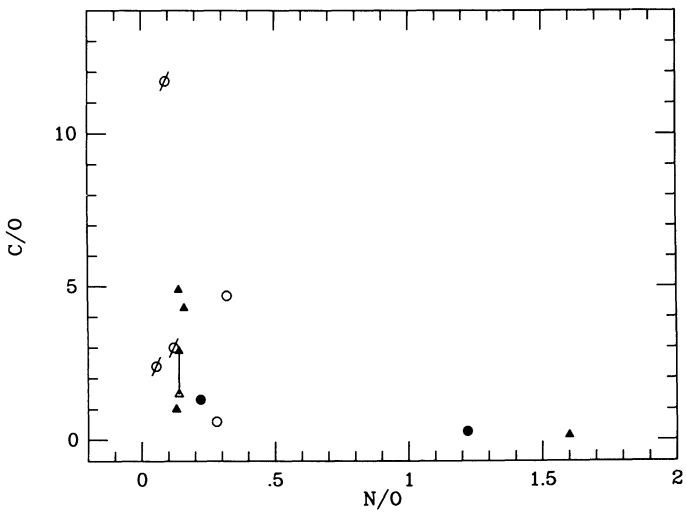

FIG. 10.—C/O plotted against N/O, with LMC and SMC objects again denoted by circles and triangles, respectively. *IUE* results are indicated by filled symbols. Nebulae with $N_e > 10^4\ \mathrm{cm}^{-3}$ are denoted by a slash. The optical and ultraviolet results for SMC/SMP 15 are again connected by a vertical bar.

3.7. *Discussion and Summary*

We must address the possibility that our temperatures might be systematically in error: see § 3.1. We have rerun the code that generates luminosities, where we recalibrate our temperatures with those derived by Dopita & Meatheringham (1990), that is, we decrease the temperatures in the low-temperature region of Figure 2 by 17% (and increase those in the middle range by 1%), and use the specific photoionization temperatures for the three objects in the upper range. Only the coolest stars show any noticeable change in core mass. It is always reduced, and generally only by a few hundredths, resulting in no change in any of the conclusions. The largest effect is for the already mentioned SMC/SMP 16 for which M_c goes from 0.89 to $0.75\ M_\odot$.

We show that our modified Stoy temperature calibration gives good and reasonable temperatures, which increases our confidence in the conclusions of KJ2. We also show that the distribution of planetary nuclei on the log L–log T plane conforms qualitatively to current views of the rates of stellar evolution and confirm the use of planetary nebulae as standard

candles for extragalactic distance determinations. From this basis follows our principal conclusion that the low-excitation nebulae—the young objects with no or little doubly ionized helium—acceptably fit the KJ1 correlations, confirming the earlier conclusion that stars with low core masses, below 0.65 $M_{\odot}$, do not (at least generally) become highly enriched in nitrogen or helium. There may be some exceptions, however. The situation for carbon is very uncertain, but the C/O ratio distribution with core mass seems at least to be consistent with that believed to exist for the carbon stars, and there is a good suggestion of an anticorrelation with N/O. What is needed now are further data on nebulae with stars of higher mass, close examination of O/H ratios, and improved data on some of the interesting anomalous objects pointed out above.

This research was supported in part by the National Science Foundation through grant AST88 13686 to the University of Illinois.

REFERENCES

Aller, L. H. 1983a, ApJ, 273, 590
———. 1983b, in IAU Symposium 103, Planetary Nebulae, ed. D. R. Flower (Dordrecht: Reidel), p. 1
Aller, L. H., & Keyes, C. D. 1987, ApJS, 65, 405
Aller, L. H., Keyes, C. D., Maran, S. P., Gull, T. R., Michalitsianos, A. G., & Stecher, T. P. 1987, ApJ, 320, 159
Aller, L. H., Keyes, C. D., Ross, J. E., & O'Mara, B. J. 1981, MNRAS, 194, 613
Boroson, T. A., & Liebert, L. 1989, ApJ, 339, 884
Ciardullo, R., Jacoby, G. H., Ford, H. C., & Neil, J. D. 1989, ApJ, 339, 53
Dopita, M. A., & Meatheringham, S. J. 1991, ApJ, 367, 115 (DM)
Henry, R. B. C., Liebert, J., & Boroson, T. A. 1989, ApJ, 339, 872
Iben, I., Jr. 1988, in Progress and Opportunities in Southern Hemisphere Optical Astronomy, ed. V. M. Blanco & M. M. Phillips (ASP Conf. Ser., 1), 220
Jacoby, G. H. 1989, ApJ, 339, 39
Jacoby, G. H., & Kaler, J. B. 1989, AJ, 98, 1662
Jacoby, G. H., Walker, A. R., & Ciardullo, R. 1990, ApJ, 365, 471
Kaler, J. B. 1976, ApJ, 210, 843
———. 1978a, ApJ, 220, 887
———. 1978b, ApJ, 226, 947
———. 1981, ApJ, 239, 78
———. 1983a, in IAU Symposium 103, Planetary Nebulae, ed. D. R. Flower (Dordrecht: Reidel), 245
———. 1983b, ApJ, 271, 188
———. 1985, ApJ, 290, 531
———. 1986, ApJ, 308, 322
Kaler, J. B., & Jacoby, G. H. 1989, ApJ, 345, 871
Kaler, J. B., & Jacoby, G. H. 1990, ApJ, 362, 491 (KJ1)
———. 1991, ApJ, 372, 215 (KJ2)
Kaler, J. B., Shaw, R. A., & Kwitter, K. B. 1990, ApJ, 359, 392
Meatheringham, S. J., & Dopita, M. A. 1991, ApJS, 75, 407 (MD)
Meatheringham, S. J., Dopita, M. A., & Morgan, D. H. 1988, ApJ, 329, 166
Monk, D. J., Barlow, M. J., & Clegg, R. E. S. 1988, MNRAS, 234, 583 (MBC)
Paczyński, B. 1971, Acta Astr., 21, 417
Renzini, A. 1979, in IAU 4th European Regional Meeting in Astronomy, Stars and Star Systems, ed. B. E. Westerlund (Dordrecht: Reidel), 155
Schönberner, D. 1981, A&A, 103, 119
Schönberner, D., & Weidemann, V. 1981, in Physical Processes in Red Giants, ed. I. Iben, Jr. & A. Renzini (Dordrecht: Reidel), 463
Shaw, R. A. 1988, in IAU Symposium 131, Planetary Nebulae, ed. S. Torres-Peimbert (Dordrecht: Kluwer), 473
Stasinska, G., & Tylenda, R. 1990, A&A, 240, 467
———. 1991, in Elements of the Cosmos, ed. R. Terlevich (Cambridge: Cambridge University Press), in press
Torres-Peimbert, S. 1983, in Stellar Nucleosynthesis, ed. C. Chiosi & A. Renzini (Dordrecht: Reidel), 3
Tylenda, R., Stasinska, G., Acker, A., & Stenholm, B. 1991, A&A, in press
Webster, B. L. 1969, MNRAS, 143, 79
———. 1983, PASP, 95, 610
Whitford, A. E. 1958, AJ, 63, 201
Wood, P. R., & Faulkner, D. J. 1986, ApJ, 307, 659
Wood, P. R., Meatheringham, S. J., Dopita, M. A., & Morgan, D. H. 1987, ApJ, 320, 178